Eur Biophys J (1998) 27: 618–625

ARTICLE

Andreas Kukol · Eberhard Neumann

Electrostatic determinants of the ion channel control of the nicotinic acetylcholine receptor of *Torpedo californica*

Received: 10 November 1997 / Revised version: 12 January 1998 / Accepted: 7 March 1998

Abstract The patch clamp K^+-conductance G of the nicotinic acetylcholine receptor (AcChoR) dimer ($M_r \approx$ 590 000) of *Torpedo californica*, reconstituted in lipid vesicles, which decreases with increasing Ca^{2+}-concentration in the range $0.1 \leq [Ca^{2+}]/mM \leq 2$, can be quantitatively rationalized by Ca^{2+}-binding to negatively charged sites, causing charge reversal reducing the normal K^+-accumulation in the channel vestibules. Cleavage of the sialic acid residues (up to 20±2 per dimer) reduces the K^+-accumulation factor $\alpha = G_0/G_\infty$ from $\alpha = 3 \pm 0.8$ of the normal AcChoR to $\alpha = 2 \pm 0.7$ for the desialyated AcChoR. Desialysation also decreases the Ca^{2+}-sensitivity of the conductance from $G_0 = 96.6 \pm 6$ pS at $[Ca^{2+}] \rightarrow 0$ of the normal AcChoR to $G_0 = 84.2 \pm 6$ pS. Endogenous hyperphosphorylation (to up to 28±4 phosphates per dimer) enhances the vestibular K^+-accumulation to $\alpha = 3.6 \pm 0.7$, without affecting the Ca^{2+}-dissociation equilibrium constant $K_{Ca} = 0.34 \pm 0.05$ mM at 295 K (22 °C). Most interestingly, even in the absence of AcCho, the hyperphosphorylated AcChoR dimer exhibits spontaneously long-lasting open channel events ($\tau = 200 \pm 50$ ms). At [AcCho] = 2 μM there are two open states ($\tau_1 = 20 \pm 10$ ms, $\tau_2 = 140 \pm 60$ ms) whereas the normal AcChoR dimer has only one open state ($\tau = 6 \pm 4$ ms). – Physiologically important is that (i) the sialic acid and phosphate residues render the AcChoR conductance sensitive to control by divalent ions and (ii) the channel behavior of the hyperphosphorylated AcChoR without AcCho appears to indicate pathophysiologically high phosphorylation activity of the cell leading, among others, to myasthenic syndromes.

Key words Acetylcholine receptor · Channel events · Sialic acids · Receptor phosphorylation

A. Kukol · E. Neumann (✉)
Fakultät für Chemie, Universität Bielefeld,
Postfach 101031, D-33501 Bielefeld, Germany
e-mail: eberhard.neumann@post.uni-bielefeld.de

I Introduction

The nicotinic acetylcholine receptor (AcChoR) is the integrative mediator in the signal transduction of cholinergic synapses, combining both receptor and primary effector protein functions. Functionally, the postsynaptic AcChoR binds the neurotransmitter acetylcholine (AcCho) which leads to a steep depolarisation of the postsynaptic membrane and ultimately to discharge of electroplaques and to muscle contraction (Fatt and Katz 1951). The nicotinic AcChoR protein is valued as one of the best characterized ion-channel proteins (see, e. g., Devillers-Thiery et al. 1993; Akabas and Karlin 1995; Hucho et al. 1996), which also serves as a model system for the fetal human AcChoR. Besides cryo-electron microscopy (Unwin 1993, 1995, 1996) no direct structural information is available. The function of specific amino acid residues of the AcChoR has been explored by site-directed mutagenesis and characterized in expression systems. Functionally, it has been previously shown that the *single channel events* of the dimer are in fact synchronous openings and closings of a *double channel* (Schindler et al. 1984; Neumann and Schürholz 1994; Neumann et al. 1996).

Here we provide novel data of the biochemically modified, affinity-purified AcChoR dimer ($M_r \approx 580\,000$) reconstituted in lipid vesicles, using the Neher-Sakmann patch clamp technique (Hamill et al. 1981; Cahalan and Neher 1992). In detail, we focus on the sialic acid residues as anionic terminal groups of the oligosaccharides (Poulter et al. 1989; Shoji et al. 1992; Nomoto et al. 1986). Further, we show that, in contrast to previous belief, the phosphate groups do modulate the channel activity and not only the desensitization behavior (Huganir et al. 1986; Huganir and Greengard 1990).

The function of the anionic groups of the AcChoR appears to be intimately linked to the binding of divalent cations. Enhanced concentrations of Ca^{2+} and Mg^{2+} reduce the K^+-conductance of the oocyte-expressed *Torpedo* AcChoR (Imoto et al. 1986, 1988) in practically the same way as the conductance of the *Torpedo* AcChoR dimer, re-

constituted in lipid vesicles (Neumann and Schürholz 1994; Neumann et al. 1996). Previously, the dramatic dependence of the channel conductance on Ca^{2+} and Mg^{2+} ions has been attributed to charge screening of the three rings of anionic amino acid residues (Imoto et al. 1988). Here we show that beyond screening there is actual *charge reversal*.

As a novelty, we show that the sialic acid residues and the phosphate groups can modulate the conductance value of the *Torpedo* AcChoR dimer in the Ca^{2+}-concentration range of $0.1 \leq [Ca^{2+}]/mM \leq 2$, where the AcChoR conductance is sensitive to changes of the anionic groups (and not screened as in the range $[Ca^{2+}] \geq 2$ mM). Additionally we find that the increase in the number of the phosphate groups causes spontaneous, long lasting open states (without the presence of AcCho), not observed with the normal AcChoR. This result may provide a key to correlate receptor hyperphosphorylation with certain pathological features of cells such as myasthenic syndromes.

II Materials and methods

Electric organ tissue from *Torpedo californica*, received on dry ice from Pacific Bio-Marine Laboratories Inc., Venice, CA was stored in liquid nitrogen. 3-[(cholamidopropyl)-dimethylammonio]-1-propansulfonate (Chaps), phenylmethanesulfonylfluoride (PMSF), Flaxedil (Gallamine-triethyliodide) and benzamidine were from Sigma; oubain, pepstatin, leupeptin, pefabloc® and sialidase were from Boehringer Mannheim, antipain and ATP from Merck KGaA, Darmstadt. The soybean lipid extract AVANTI 20 was from AVANTI Polar Lipids Inc., the 400 nm polycarbonatmembrane from Avestin and the dicaproyl-MP (N-6-aminocaproyl-6′-aminocaproyl-3-aminopyridiniumbromid)/sepharose 4B affinity column was a generous gift from Prof. H. W. Chang, Columbia University, New York.

Preparation of the AcChoR-dimer. The AcChoR dimer is prepared as described, e. g., by Neumann and Schürholz (1994). In brief, the frozen *Torpedo* electric organ was homogenized and centrifugated. The membrane proteins were extracted from the resuspended pellet by 1% (by weight) CHAPS. After separation of the nonsolubilized material by centrifugation the supernatant is applied to the dicaproyl-MP/sepharose 4B affinity column, eluted with flaxedile and stored at –70 °C.

Preparation of lipid vesicles. The soybean phospholipids were dissolved in chloroform together with 10% cholesterol (by weight). After evaporation of chloroform the lipid was suspended in 10 mM HEPES pH 7.4, 500 mM NaCl, 2 mM $CaCl_2$, 0.02% NaN_3 to a content of 20 mg/ml and subjected five times to a freezing-thawing cycle. Immediately before use the lipid suspension was extruded through a 400 nm polycarbonate membrane eleven times.

Reconstitution to lipid vesicles. The solubilized *Torpedo* AcChoR was mixed with solutions of $CaCl_2$, NaCl, CHAPS and extruded lipid to yield the final concentrations of 500 mM NaCl, 2 mM $CaCl_2$, 10 mg/ml lipid, 3.4 mg/ml CHAPS and an AcChoR content of 0.4 mg/ml. The turbid suspension was shaken 12 h at 4 °C and subsequently dialyzed 64 h in 0.5 M NaCl, 10 mM HEPES pH 7.4, 2 mM $CaCl_2$, 0.02% NaN_3 and 24 h in 100 mM NaCl without $CaCl_2$.

Sialic acid test. The standard spectrophotometric sialate test was performed as described by Warren (1959) and Amidoff (1961) with modifications reported by Manzi and Varki (1993). The numerical values and error margins refer to three independent determinations.

Phosphate test. The standard spectrophotometric test was performed as described by Buss et al. (1983) with the following modification: the precipitate was washed three times with ethanol/diethylether (1 : 1 by volume) to remove associated phospholipids. The data represent mean values of three independent determinations.

Integral Li^+-Influx. The global ion-transport activity of the reconstituted AcChoR was measured by the acetylcholine induced Li^+-uptake into reconstituted vesicles. The Li^+ assay was analogous to that with vesicular membrane fragments (Bernhardt et al. 1981). The vesicles were dialyzed 16 h in 10 mM HEPES pH 7.4, 145 mM sucrose, 0.02% NaN_3 at 4 °C. For the flux assay, samples of 115 µl vesicles were mixed with 5 µl of 2 M LiCl and 2.5 µl of 5 mM acetylcholine. In the control experiments buffer solution substitutes the acetylcholine solution. The external Li^+ was separated from the vesicles by passage through a 1.5 ml Dowex 50 WX-8-100 cation exchange column preequilibrated with 3 ml 170 mM sucrose, 3.3 mg/ml bovine serum albumin. The column was immediately eluted with 1.6 ml 175 mM sucrose solution and the elutant was analyzed by atomic emission spectroscopy (AES) at 670 nm (Unicam SP 1900). The numerical values refer to 3 independent determinations.

Patch-clamp measurements. The channel activity of inside-out patches of the vesicle reconstituted AcChoR dimer was measured using the amplifier L/M-EPC 7 (List, Darmstadt). The data were stored after filtering at 1 kHz (3-pole bessel filter) and digitizing at 4.166 kHz with Digidata 1200 (Axon Instruments) directly on the hard disc of the computer (Intel Pentium based system). The channel currents measured at positive pipette-potential appear as upward openings in the channel traces (and correspond to a cellular inward current through the AcChoR in this inside-out configuration). The bath solution contained 10 mM K-HEPES pH 7.4, 100 mM KCl, 0.01% NaN_3 and varying concentrations of $CaCl_2$. The pipette solution was the same as the bath solution, except that 2 µM acetylcholine was added. The temperature was 295 K (22 °C).

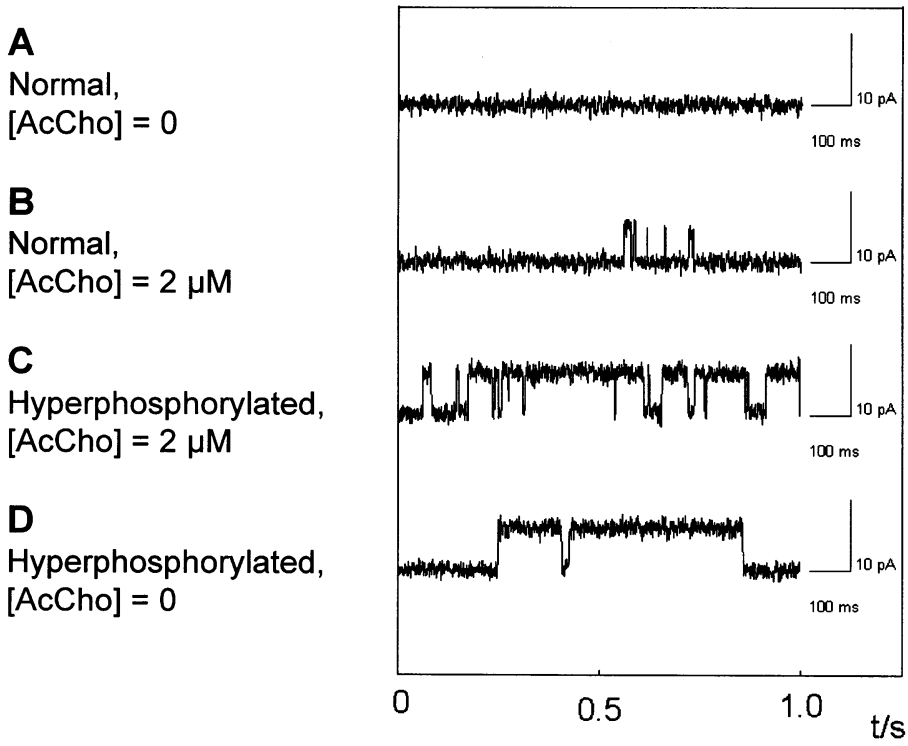

Fig. 1 A–D Recordings (current/time traces) of single channel events of the lipid vesicle-reconstituted *Torpedo* AcChoR dimer (under patch clamp conditions). Buffer: [KCl] = 100 mM, [$CaCl_2$] = 0.5 mM, [HEPES] = 10 mM, pH 7.4, 0.01% NaN_3, at T = 295 K (22 °C) and [AcCho] as indicated. **A** Normal AcChoR dimer at V = +80 mV, no AcCho. **B** Normal AcChoR dimer at V = +80 mV, [AcCho] = 2 µM. **C** Hyperphosphorylated AcChoR dimer at V = +100 mV, [AcCho] = 2 µM. **D** Hyperphosphorylated AcChoR dimer at V = +100 mV, no AcCho present

Data analysis. The current/time traces were analyzed with the numerical software system Matlab™ (Mathworks Inc.) and the Ion-Channel Toolbox for Matlab™ (available from *http://www.mathworks.com.physicv4.html*). Firstly, the base line of the current trace was corrected and filtered digitally at f_c = 500 Hz (3 dB cut off frequency). The channel current was obtained by Gaussian fitting of amplitude distributions, the open-closed times by double threshold detection. After correction for the filter response, the integral open time distribution $F(t)$ is obtained by summing the differential distribution $f(t)$ according to

$$F(t) = \int_t^\infty f(t)dt = \sum_{i=1}^{n} a_i \cdot \exp(-t/\tau_i),$$

where a_i is the relative amplitude of the i-th contribution ($1 \le i \le n$). The integral open-time (t_0, Fig. 3) distribution is fitted by a sum of exponentials given by the right hand side of the equation with the time constants τ_i (Colquhoun and Hawkes 1995). Although fitting the integral time distribution is very erroneous because the successive data points are highly correlated (Colquhoun and Sigworth 1995), it is only in this form of distribution that exponential components are visible; the number of channel events must be necessarily low in order to avoid overlaps of the channels events. The open-time histograms are built with the binwidth set to 1 ms, such that the minimal time resolution is $\Delta t > 1$ ms.

III Results

We have found that the sialic acid content of the AcChoR dimer can be reduced by sialidase treatment from normally 19 (±2) residues to 1 (±1) residue. The desialyated AcChoR shows the same global Li^+-ion transport activity (28±4%) (Bernhardt et al. 1981; Neumann et al. 1996) as the lipid vesicle-reconstituted, normal protein with intact sialic acid groups, which releases 25±4% of the entrapped Li^+ upon addition of AcCho. The hyperphosphorylated AcChoR, however, already releases the Li^+ in the absence of AcCho such that the remaining, AcCho-inducible release is only 6±2% of the initial normal Li^+ content.

In patch clamp the overall pattern of the channel activity of the desialyated AcChoR is very similar to that of the normal AcChoR, both elicited by 2 µM AcCho: isolated channel openings or clusters of three to ten openings (Fig. 1). However, compared to the normal AcChoR, the K^+-conductance of the desialyated AcChoR decreases less strongly when the Ca^{2+} content increases from 0.1 mM to 2.0 mM (Fig. 2 A).

The normal AcChoR has only 14±4 phosphate groups per dimer (prepared without the inhibition of phosphatases). The phosphorylation of the AcChoR, when still in *Torpedo* electrocyte membrane fragments, by the endogenous kinase activity in the presence of the phosphatase inhibitor F^-, increases the number of phosphate groups up to 28±4 per AcChoR dimer. Functionally, this hyperphosphorylation results in a slight asymmetry of the current-voltage relationship. For instance, at [Ca^{2+}] = 0.1 mM (Fig. 2 B), the (cellular) inward current conductance is G = 91±4 pS whereas the outward conductance is G = 84±4 pS, compared to G = 81±4 pS of the normal AcChoR dimer (which within the experimental error is independent of the direction); see below.

More dramatically, hyperphosphorylation appreciably affects the opening-closing kinetics of the protein channel.

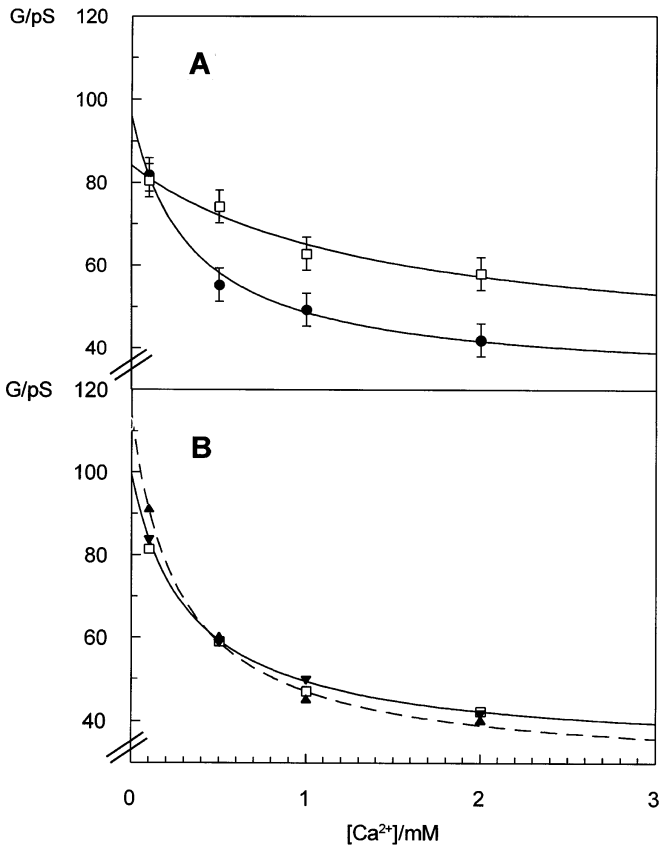

Fig. 2 A, B Dependence of the K^+-conductance G of the lipid vesicle-reconstituted *Torpedo* AcChoR dimer on the concentration of $[Ca^{2+}]$. **A** ● normal AcCho dimer; □ desialyated AcChoR dimer. The conductance G is obtained from the *linear current* (I) – voltage (V) relationship in the range of V = –100 mV to +100 mV from inside-out patches as G = I/V at the buffer conditions: [KCl] = 100 mM, [HEPES] = 10 mM, pH 7.4, 0.01% NaN_3, T = 295 K (22 °C) and additionally [AcCho] = 2 μM in the pipette. **B** □ normal AcChoR-dimer; – –▲– – hyperphosphorylated dimer (*inward current*), —▼— hyperphosphorylated dimer (*outward current*). For the normal AcChoR the current-voltage relation is linear in the range of –100 mV to +100 mV. Error bars are omitted for clarity. Buffer conditions as in A. The continuous curves refer to curves by Eq. (2) of the text

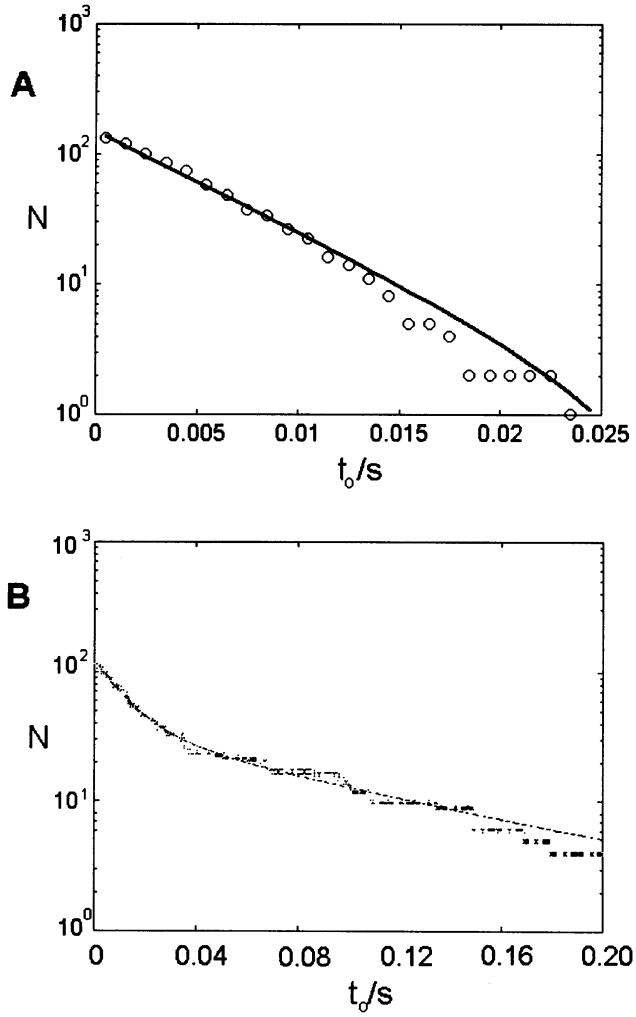

Fig. 3 A, B Integral open-time (t_0) distribution of the lipid vesicle reconstituted AcChoR dimer with logarithmic y-axis. The number of the summed opening events N were build up from 1 ms time intervals (conditions: [KCl] = 100 mM, $[CaCl_2]$ = 0.5 mM, [HEPES] = 10 mM, pH 7.4, 0.01% NaN_3 [AcCho] = 2 μM, V = –100 mV). **A** Normal AcChoR dimer integral open-time distribution fitted with one exponential with the mean open time τ = 5.7 ms. **B** Hyperphosphorylated AcChoR dimer, integral open-time distribution fitted with two exponentials τ_1 = 25 ms with the mean open times and τ_2 = 90 ms, respectively

The hyperphosphorylated AcChoR shows AcCho-induced long lasting open states with mean dwell-times in the range of τ = 0.15 s and short open states with mean dwell-times in the ms time range (Fig. 1 C). The normal AcChoR, on the other hand, exclusively exhibits the short type of openings.

The picture emerging from visual inspection of the channel records can be quantified by statistic analysis of the open times; exponential fitting yields integral open-time distributions. The hyperphosphorylated AcChoR at [AcCho] = 2 μM exhibits *two* components with mean open-times τ_1 = 20±10 ms and τ_2 = 140±60 ms, respectively, whereas the normal AcChoR shows only *one* component with τ = 6±4 ms (Fig. 3). The relatively large error margins result from the relatively small number of channel events of the lipid vesicle reconstituted *Torpedo* AcChoR, caused by the limited lifetime of an intact patch (maximum of 5 min).

The closed-time distribution always shows two time constants; the larger one, varies between 0.9 s and 10 s. The closed-times are not further discussed because free diffusion of one or more receptors in and out of the patched area cannot be ruled out.

The most remarkable new result, however, is that the hyperphosphorylated AcChoR *opens spontaneously without the presence of the neurotransmitter AcCho* (Fig. 1 D). The open-time distribution of this spontaneous openings can be fitted by *one* exponential with τ = 200±50 ms, compared with τ_2 = 140±60 ms in the presence of AcCho (Fig. 1 C). The conductance value of this open state and its Ca^2-dependence is practically the same as that in the presence of acetylcholine.

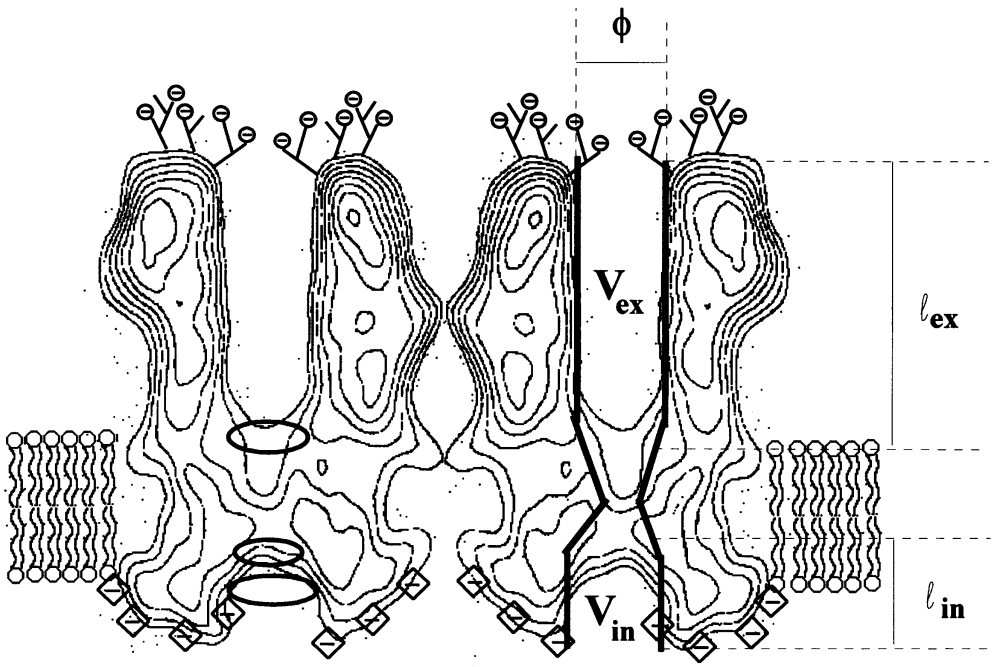

Fig. 4 Cross section of the *Torpedo* AcChoR dimer drawn on the basis of cryoelectron microscopic data of Unwin (1993). We have introduced the possible location of the three anionic rings (Imoto et al. 1986) in one of the monomer fragments, the sialic acid residues (⊖, this study) and the additional (hyper-)phosphate groups (⟐, this study). In the right hand side monomer fragment the dimensions of the cylinder model are given: $\phi = 2$ nm, $l_{ex} = 6.6$ nm, $l_{in} = 2.0$ nm with $A_{ex} = \pi \cdot l_{ex} \cdot \phi = 42$ nm^2 and $A_{in} = 13$ nm^2. See also Table 1

IV Theory and discussion

It is worth noting that the Ca^{2+} concentration dependence of the K^+-channel conductance of the normal, desialyated and hyperphosphorylated AcChoR, respectively, can be interpreted by the same physico-chemical model: the negatively charged groups of the proteins attract cations and, especially, accumulate monovalent cations in and near the channel vestibules (Fig. 4). Therefore, the conductance value is raised in comparison to that in the presence of less anionic charges. The conductance reduction by Ca^{2+} (and Mg^{2+}, data not shown) has been previously attributed to the shielding of the negative charges (Imoto et al. 1986; Neumann et al. 1996). Specifically, the Ca^{2+}-ions may just contribute to the ionic atmosphere screening of the negatively charged sites according to the Debye-Hückel concept. But, because at $[Ca^{2+}] \leq 1$ mM the screening will be dominated by the (highly concentrated) K^+-ions (100 mM), direct binding of Ca^{2+} to negatively charged sites R is more realistic (see also below).

The Ca^{2+}-binding model

If the binding sites are considered as independent, we can apply the simple binding scheme according to:

$$Ca^{2+} + R^- \rightleftharpoons CaR^+, \tag{1}$$

where R^- is an anionic binding site, CaR^+ the occupied site (with charge reversal) and $K_{Ca} = [Ca^{2+}] \cdot [R^-]/[CaR^+]$ is the apparent equilibrium dissociation constant.

Since the channel conductance is proportional to the concentration of mobile ions (here K^+) which are accumulated by the R^--groups and repelled by the CaR^+-sites, we can safely assume that the relationship between the conductance G and the fraction $\beta = ([R^-]\text{-}[CaR^+])/[R_t]$ of the remaining negative charges, accumulating the mobile transported cations, is linear (Neumann and Schürholz 1994; Neumann et al. 1996), where $[R_t] = [R^-] + [CaR^+]$ is the total concentration of sites. Therefore, we have $\beta = (G - G_x)/(G_0 - G_x)$ and obtain the suggestive expression:

$$G = G_i \cdot \frac{[R^-] - [CaR^+]}{[R_t]} + G_x \tag{2}$$

If the conductance at $[Ca^{2+}] \rightarrow 0$ is denoted by $G_0 = G_i + G_x$ and the saturation (minimum) value is denoted by $G_\infty = G_x - G_i$, where G_i is the mean conductance contribution of the anionic Ca^{2+}-binding sites and G_x is an additive constant (which finally drops out), Eq. (2) is rearranged to:

$$G = (G_0 - G_x) \cdot \left(1 - 2\frac{[Ca^{2+}]}{[Ca^{2+}] + K_{Ca}}\right) + G_x \tag{3}$$

Data fit (Fig. 2) with Eq. (3) yield the parameters G_0, G_∞ and K_{Ca}, respectively (Table 1). The desialyated AcChoR dimer (Fig. 2) exhibits a smaller G_0 (in the absence of Ca^{2+}), an enhanced G_∞ and a fourfold higher Ca-dissociation constant ($K_{Ca} = 1.4 \pm 0.1$ mM) in comparison with that of the normal AcChoR ($K_{Ca} = 0.34 \pm 0.05$ mM). At $[Ca^{2+}] \geq 0.5$ mM the conductance of the desialyated AcChoR is higher than that of the normal AcChoR. Note that $K_{Ca} = 0.34 \pm 0.05$ mM at $T = 295$ K (22 °C) is equal to $K_{Ca} = 0.33$ mM at $T = 293$ K (20 °C) derived from direct titration of AcChoR-lipid-detergent micelles (Chang and Neumann 1976; Rübsamen et al. 1976).

The data (Fig. 2) indicate that the sialic acid residues, indeed, do contribute to the Ca^{2+}-binding, although they are probably located only on the mouth of the extracellu-

Table 1 Limit conductances G_0 and G_∞, at $[Ca^{2+}] = 0$ and $[Ca^{2+}] \to \infty$, of the Torpedo AcChoR dimer and electrostatic model parameters at T = 295 K (22 °C)

AcChoR dimer	G_0/pS	G_∞/pS	K_{Ca}/mM	α	$-\Psi_0$/mV	$\sigma/(-e_0 \cdot nm^{-2})$	$N(V_{ex})$	N_{tot}
Normal	96±6	32±5	0.34±0.05	3±0.8	28±2	0.13 ±0.05	11	14.2
Desialyated	84±6	39±5	1.4 ±0.5	2±0.7	20±2	0.094±0.005	8	10.3
Hyperphosphorylated								
Inward current	99±6	33±5	0.33±0.05	3±0.7	35±3	0.17 ±0.03	14.3	18.7
Outward current	114±8	29±5	0.27±0.04	3.6±0.7	40±4		4.4*	

Data evaluation of the reaction $CaR^+ \rightleftharpoons R^- + Ca^{2+}$ where R^- refers to an anionic Ca^{2+}-binding site, K_{Ca} is the Ca^{2+}-dissociation equilibrium constant and $\alpha = G_0/G_\infty = [K^+_{in}]/[K^+_{ex}]$ the vestibular accumulation factor. The parameters were obtained with Eq. (2) and Eq. (3) of the text. Conditions are the same as those given in Fig. 2. The surface potential Ψ_0, the surface charge density σ and number of excess anionic groups $N(V_{ex})$ in the external receptor vestibule of cylinder volume V_{ex}, cylinder internal surface $A_{ex} = 42\ nm^2$, and $N(V_{in})$ in the cytosolic vestibule of V_{in} and surface $A_{in} = 13\ nm^2$, with $V_{tot} = V_{ex} + V_{in}$, $A_{tot} = A_{ex} + A_{in}$ and $N_{tot} = N(V_{in}) + N(V_{ex})$, all refer to the electrostatic cylinder model; see Fig. 4. The value 4.4* refers to the cytosolic vestibule, $N(V_{in})$

lar vestibule; but they actually lead to a *reversal of the polarity* of the binding site at higher $[Ca^{2+}]$. Such a charge reversal cannot be due to simple Debye-Hückel shielding, it can only result from binding. Note that the charge reversal requires a theoretical "Ansatz" which is different from previous analyses (see, e. g. Neumann et al. 1996). Physiologically important is that in the normal AcChoR the sialic acid residues enhance the Ca^{2+}-sensitivity of the ion transport, thus providing an effective control of the conductance of the AcChoR by extracellular calcium and intracellular Mg^{2+} ions.

The effect of hyperphosphorylation on the K^+-conductance in the range $0.1 \le [Ca^{2+}]/mM \le 2$ is less obvious. In terms of our Ca^{2+}-binding model, hyperphosphorylation enhances the channel outward-conductance at low intracellular Ca^{2+}-concentration. This new result has remained obscured so far, because most single channel measurements are carried out at relatively high concentrations of divalent cations ($[Ca^{2+}] = 2$ mM, $[Mg^{2+}] = 2$ mM), where the Ca^{2+}-sensitivity is already saturated (Fig. 2). As to the asymmetry of the outward and inward current of the hyperphosphorylated AcChoR (Fig. 2 B), the additional phosphate groups lead to a higher density of R^--groups in the intracellular vestibule. This, in turn, results in a more effective Ca^{2+}-binding (polyelectrolyte effect). Thereby K^+-accumulation is reduced and the outward current is increased to a smaller extent than the inward current.

The electrostatic determinants of the *Torpedo* AcChoR dimer

The limiting conductance parameters G_0 and G_∞ may also be used in terms of the electrochemically well established relationship between conductance and ion concentrations, here $G \propto [K^+]$. Specifically, we apply the simple Boltzmann-"Ansatz" for the ratio G_0/G_∞ defining the ion accumulating factor α by:

$$\alpha = \frac{G_0}{G_\infty} = \frac{[K^+]_{in}}{[K^+]_o} = \exp\left(\frac{-z_K F \Delta\Psi}{RT}\right) \quad (4)$$

where $z_K = +1$ is the charge number of the dominantly transported K^+ ion, $[K^+]_{in}$ the concentration of the K^+-ions accumulated in the receptor vestibules and $[K^+]_o$ that of the bulk solution; F is the Faraday constant, R the gas constant and T the absolute temperature. For the normal AcChoR dimer we obtain $\alpha = 3 \pm 0.8$, suggesting that the local vestibular K^+-concentration in the absence of Ca^{2+} is three times larger than in the bulk. For the desialyated receptor we find $\alpha = 2 \pm 0.7$; hence the K^+-ion accumulation is smaller than normal.

In Eq. (4), the electric potential difference $\Delta\Psi = \Psi_\infty - \Psi_0$ refers to the unscreened value Ψ_0 and the totally screened value $\Psi_\infty \approx 0$. Hence we may set $\Delta\Psi = \Psi_0$. With Eq. (4) we obtain for the normal AcChoR: $\Psi_0 = -28 \pm 2$ mV and for the desialyated AcChoR: $\Psi_0 = -20 \pm 2$ mV; both values reflect the excess of anionic groups on the receptor surface.

Finally, we apply the Grahame equation (Grahame 1947) for the surface charge density (σ) in the form of

$$\sigma^2 = 2\ RT \varepsilon_0 \varepsilon_r \Sigma\ c_j \cdot \exp\left[-z_j F\ \Psi_0/RT\right] \quad (5)$$

where ε_0 is the vacuum permittivity, ε_r the dielectric constant (here $\varepsilon_r = \varepsilon_{Water} = 80$ at 295 K) and $j = K^+, Cl^-$. Thus $z_K = +1$ and $z_{Cl} = -1$ and $c_j = [K^+]_0, [Cl^-]_0$. The numerical values of Ψ_0, σ in units of the (positive) elementary charge e_0 and the mean number N of excess anionic groups affecting the receptor conductance can be estimated in terms of a simple cylinder model, sketched in Fig. 4 for one of the receptor monomer fragments ($M_r \approx 290\,000$); see Table 1. The desialyated AcChoR dimer has about $\Delta N_{tot} = 4$ excess charges less than the normal AcChoR. Since there are 20±4 sialic acid residues per dimer the contribution of only 4 anionic excess charges to the charge pattern of the vestibules ($V_{tot} = V_{ex} + V_{in}$) reflects the surface position of the sugar residues.

The open-closed switching of the hyperphosphorylated AcChoR channel is very different from that of the normal AcChoR. It is recalled that the open-time distribution reveals two time constants ($\tau_1 = 20 \pm 10$ ms and $\tau_2 = 140 \pm 60$ ms). If this result is interpreted in terms of the "Hidden Markov Model" of channel kinetics (e. g. Ball and Rice 1992), the hyperphosphorylated AcChoR must have two distinct open states. The hyperphosphorylation modifies the protein structure such that an additional open state becomes appreciably populated. This additional open state

is *independent of the presence of the agonist acetylcholine* because the channel opens even in the absence of acetylcholine with the mean open-time $\tau = 200 \pm 50$ ms. Therefore, the minimal reaction scheme of the AcChoR activation (Edmonds et al. 1995) must be extended and contain the AcCho independent open state R*R* (scheme 6):

$$2A + \begin{bmatrix} RR \\ \Updownarrow \\ R^*R^* \\ \Updownarrow \\ DD \end{bmatrix} \rightleftharpoons A + \begin{bmatrix} AR_2 \\ \Updownarrow \\ AR^* \cdot R \\ \Updownarrow \\ AD \cdot D \end{bmatrix} \rightleftharpoons \begin{bmatrix} A_2R_2 & \text{(closed)} \\ \Updownarrow & \\ A_2R_2^* & \text{(open)} \\ \Updownarrow & \\ A_2D_2 & \text{(desensitized)} \end{bmatrix} \quad (6)$$

The data of Rauer et al. (1996) and Chang et al. (1984) suggest that the AcChoR dimer (RR) binds cooparatively two molecules of acetylcholine upon activation; see also Neumann et al. (1996). Whereas synchronous opening-closing channel events due to double-channels of the dimer have been observed previously (Schindler et al. 1984; Neumann et al. 1996), channel openings without agonists are rare (Jackson 1986, 1988); but these openings become more frequent upon AcChoR hyperphosphorylation with protein kinase A (Ferrer-Montiel et al. 1991). Oocyte expression of the *Torpedo* AcChoR lacking the γ-subunit also shows an increase in the frequency of spontaneous channel openings (Jackson et al. 1990) Hence the unliganded open state R*R* also exists in the normal receptor, but in very low concentration.

The Monod-Wyman-Changeux limit model for allosteric transitions (Monod et al. 1965; Eigen 1967) has been successfully applied to ligand-gated membrane receptors in order to describe the macroscopic concentration-response curves as well as channel events (Edelstein et al. 1996). The conformer R*R* is obviously stabilized by the high degree of hyperphosphorylation, as also achieved here. The electrostatic repulsion of the phosphate groups probably introduces tensions in the protein molecule which readily relax to yield the open channel state. Additionally, as elaborated by Urry (1993), phosphorylation introduces ionic hydration at the expense of (formerly) hydrophobic hydration. If this also occurs in the hyperphosphorylated AcChoR, it may result in enhanced contacts between hydrophobic regions of the AcChoR.

Finally, we may address the potential pathophysiological relevance of the hyperphosphorylation and the spontaneous long lasting open states. In the case of the phosphorylation of the AcChoR by protein kinase A (Ferrer-Montiel et al. 1991) or addition of cAMP to embryonal chicken muscle cells (Kolb and Wakelam 1983) only the short type of AcChoR channel openings has been observed. DNA cloning from patients who suffer from the myasthenia syndrome reveals that there is the point-mutation εThr264Pro (Ohno et al. 1995). If this mutated DNA is expressed in human embryonic kidney fibroblasts, one observes the appearence of long lasting open states (with $\tau = 73$ ms) evoked by acetylcholine. Long-lasting open events of the AcChoR are therefore a potential indicator of pathophysiological hyperphosphorylation activity in nerve and muscle cells.

It is instructive to compare the effect of phosphorylation of the *Torpedo* electric organ AcChoR with that of other ligand-gated receptor channels of the type-I receptor family such as the brain γ-aminobutyric type A ($GABA_A$) receptor channels (Schofield et al. 1987) or the glycine receptor channels (Grenningloh et al. 1987).

Whereas the nicotinic AcChoR is a cation specific channel protein for the neuromuscular signal activation, the $GABA_A$ channel protein, for instance, is a synaptic inhibitory chloride channel. The channel activity of $GABA_A$ and N-methyl-D-aspartate (NMDA) receptor channels is also modulated by phosphorylation and there are spontaneous current activities in the absence of ligands; see, e. g., E. Sigel (1995), Jones and Westbrook (1997). Up to now, to our knowledge, the number of phosphate groups, the organization as monomeric or dimeric receptor species as well as hyperpolarization was not yet specified as in the case of AcChoR.

Acknowledgements We thank Ina Ehring for excellent technical assistance, Marlies Hofer for careful processing of the compuscript and we gratefully acknowledge partial support by the Deutsche Forschungsgemeinschaft DFG-grants SFB 223/C01 and Ne 227/9-1 to E. Neumann.

References

Akabas MH, Karlin A (1995) Toward a structural basis for the function of nicotinic acetylcholine receptors and their cousins. Neuron (Cambridge Ma) 15: 1231 – 1244

Aminoff D (1961) Methods for the quantitative estimation of N-acetylneuraminic acid and their application to hydrolysates of sialomucoids. Biochem J 81: 384 – 389

Ball FG, Rice JA (1992) Stochastic models for ion channels: introduction and bibliography. Math Biosci 112: 189 – 206

Bernhardt J, Moss KM, Luckinger RM, Neumann E (1981) Preparation of sealed *Torpedo marmorata* membrane fragments suitable for quantitative tracer flux studies. FEBS Lett 134: 245 – 248

Cahalan M, Neher E (1992) Patch clamp techniques: an overview. Methods Enzymol 207: 3 – 13

Chang HW, Neumann E (1976) Dynamic properties of isolated acetylcholine receptor proteins: Release of calcium ions caused by acetylcholine binding. Proc Natl Acad Sci USA 73: 3664 – 3667

Chang HW, Bock E, Neumann E (1984) Long-lived metastable states and hysteresis in the binding of acetylcholine to *Torpedo californica* acetylcholine receptor. Biochemistry 23: 4546 – 4556

Devillers-Thiery A, Galzi JL, Eisele JL, Bertrand S, Bertrand D, Changeux J-P (1993) Functional architecture of the nicotinic acetylcholine receptor: Prototype of ligand – gated ion channels. J Membrane Biol 136: 97 – 112

Edelstein SJ, Schaad O, Henry E, Bertrand D, Changeux J-P (1996) A kinetic mechanism for nicotinic acetylcholine receptors based on multiple allosteric transitions. Biol Cybernetics 75: 361 – 379

Edmonds B, Gibb AJ, Colquhoun D (1995) Mechanisms of activation of muscle nicotinic acetylcholine receptors and the time course of endplate currents. Annu Rev Physiol 57: 469 – 493

Eigen M (1967) Fast reactions and primary processes in chemical kinetics. In: Claesson S (ed) Nobel Symposium 5. Interscience Publ, Stockholm, pp 333 – 369

Fatt P, Katz B (1951) Analysis of the endplate potential recorded with an intracellular electrode. J Physiol (Lond) 115: 320 – 370

Ferrer-Montiel A, Montal MS, Diaz-Munoz M, Montal M (1991) Agonist-independent activation of acetylcholine receptor channels by protein kinase A phosphorylation. Proc Natl Acad Sci USA 88: 10 213 – 10 217

Grahame DC (1947) The electric double layer and the theory of electrocapillarity. Chem Rev 41: 441 – 501
Grenningloh G, Rienitz A, Schmitt B, Methfessel C, Zensen M, Beyreuther K, Gundelfinger ED, Betz H (1987) The strychnine-binding subunit of the glycine receptor shows homology with nicotinic acethylcholine receptors. Nature 328: 215 – 220
Hamill OP, Marty A, Neher E, Sakmann B, Sigworth FJ (1981) Improved patch clamp techniques for high-resolution current recording from cells and cell-free membrane patches. Pflügers Arch 391: 85 – 100
Hucho F, Tsetlin VI, Machold J (1996) The emerging three-dimensional structure of a receptor: the nicotinic acetylcholine receptor. Eur J Biochem 239: 539 – 557
Huganir RL, Delcour AJ, Greengard P, Hess GP (1986) Phosphorylation of the nicotinic acetylcholine receptor regulates its rate of desensitization. Nature 321: 774 – 776
Huganir RL, Greengard P (1990) Regulation of neurotransmitter receptor desensitization by protein phosphorylation. Neuron 5: 555 – 567
Imoto K, Methfessel C, Sakmann B, Mishina M (1986) Location of a δ-subunit region determining ion transport through the acetylcholine receptor channel. Nature 324: 670 – 674
Imoto K, Busch C, Sakmann B, Mishina M, Konno T, Nakai J, Bujo H, Mori Y, Fukuda K, Numa S (1988) Rings of negatively charged amino acids determine the acetylcholine receptor channel conductance. Nature 335: 645 – 648
Jackson MB (1986) Kinetics of unliganded acetylcholine receptor channel gating. Biophys J 49: 663 – 672
Jackson MB (1988) Dependence of acetylcholine receptor channel kinetics on agonist concentration in cultured mouse muscle fibers. J Physiol 397: 555 – 583
Jackson MB, Imoto K, Mishina M, Konno T, Numa S, Sakmann B (1990) Spontaneous and agonist-induced openings of an acetylcholine receptor channel composed of bovine muscle α-, β- and δ-subunits. Eur J Physiol Pflügers Arch 417: 129 – 135
Jones MV, Westbrook GL (1997) Shaping of IPSCs by endogenous calcineurin activity. J Neurosci 17: 7626 – 7633
Manzi AE, Varki A (1993) Compositional analysis of glycoproteins. In: Fukuda M, Kobata A (eds) Glycobiology – A practical approach. Oxford University Press, Oxford, UK, pp 27 – 43
Monod J, Wyman J, Changeux J-P (1965) On the nature of allosteric transitions: a plausible model. J Mol Biol 12: 88 – 118
Neumann E, Weber J, Schürholz T (1996) The initiation of the muscle action potential. Arch Physiol Biochem 104: 731 – 744
Neumann E, Schürholz T (1994) The electrochemical signal transmission by the acetylcholine receptor: Single channel conductance events and oligochannels. In: Melandri BA, Milazzo G, Blank M (eds) Bioelectrochemistry. Plenum Press, New York, pp 195 – 217
Nomoto H, Takahashi N, Nagaki Y, Endo S, Arata Y, Hayashi K (1986) Carbohydrate structures of acetylcholine receptor from *Torpedo californica* and distribution of oligosaccharides among the subunits. Eur J Biochem 157: 232 – 242
Ohno K, Hutchinson DO, Milone M, Brengman JM, Bouzat C, Sine SM, Engel AG (1995) Congenital myasthenic syndrome caused by prolonged acetylcholine receptor channel openings due to a mutation in the M2 domain of the ε-subunit. Proc Natl Acad Sci USA 92: 758 – 762
Poulter L, Earnest JP, Stroud RM, Burlingame AL (1989) Structure, oligosaccharide structures and posttranslationally modified sites of the nicotinic acetylcholine receptor. Proc Natl Acad Sci USA 86: 6645 – 6649
Rauer B, Neumann E, Widengren J, Rigler R (1996) Fluorescence correlation spectrometry of the interaction kinetics of tetramethylrhodamin alpha-bungarotoxin with *Torpedo californica* acetylcholine receptor. Biophys Chem 58: 3 – 12
Rübsamen H, Hess GP, Eldefrawi AT, Eldefrawi ME (1976) Interaction between calcium and ligand binding sites of the purified acetylcholine receptor studied by use of a fluorescent lanthanide. Biochem Biophys Res Commun 68: 56 – 63
Schindler H, Spillecke F, Neumann E (1984) Different channel properties of *Torpedo* acetylcholine receptor monomers and dimers reconstituted in planar membranes. Proc Natl Acad Sci USA 18: 6222 – 6226
Schofield PR, Darlison MG, Fujita N, Burt DR, Stephenson FA, Rodriguez II, Rhee LM, Ramachandran J, Reale V, Glencorse TA, Seeburg PH, Barnard EA (1987) Sequence and functional expression of the $GABA_A$ receptor shows a ligand-gated receptor super-family. Nature 328: 221 – 227
Shoji H, Takahashi N, Nomoto H, Ishikawa M, Shimada I, Arata Y, Hayashi K (1992) Detailed structural analysis of asparagine-linked oligosaccharides of the nicotinic acetylcholine receptor from *Torpedo californica*. Eur J Biochem 207: 631 – 641
Sigel E (1995) Functional modulation of ligand-gated $GABA_A$ and NMDA receptor channels by phosphorylation. J Receptor Signal Transduction Res 15: 325 – 332
Unwin N (1993) Nicotinic acetylcholine receptor at 9 A resolution. J Molecular Biology 229: 1101 – 1124
Unwin N (1995) Acetylcholine receptor channel imaged in the open state. Nature 373: 37 – 43
Unwin N (1996) Projection structure of the nicotinic acetylcholine receptor: Distinct conformations of the α subunits. J Mol Biol 257: 586 – 596
Urry DW (1993) Molecular machines: how motions and other functions of living organisms can result from reversible chemical changes. Angew Chem Int Ed English 32: 819 – 841
Warren L (1959) The thiobarbituric acid assay of sialic acids. J Biol Chem 234: 1971 – 1975